

# NON-LINEAR NUMERICAL MODELING OF DIP-SLIP FAULTS FOR STUDYING GROUND SURFACE DEFORMATION

Pradeep Kumar RAMANCHARLA<sup>1</sup> and Kimiro MEGURO<sup>2</sup>

<sup>1</sup>Ph.D. Student, Institute of Industrial Science, The University of Tokyo  
(4-6-1 Komaba, Meguro-Ku, Tokyo 153-8505, Japan, [pradeep@incede.iis.u-tokyo.ac.jp](mailto:pradeep@incede.iis.u-tokyo.ac.jp))

<sup>2</sup>Dr. of Eng., Assoc. Professor, Institute of Industrial Science, The University of Tokyo  
(4-6-1 Komaba, Meguro-Ku, Tokyo 153-8505, Japan, [meguro@incede.iis.u-tokyo.ac.jp](mailto:meguro@incede.iis.u-tokyo.ac.jp))

1999年に発生したトルコ・コジャエリ地震や台湾・集集地震では、地震断層運動による表層地盤の変状が、多くの土木・建築構造物に甚大な被害を与えた。本研究は、破壊現象を高精度に追跡できる応用要素法(AEM: Applied Element Method)を用いたシミュレーションから、断層運動が表層地盤に与える影響を分析するものである。地下の断層運動が地表地盤に与える影響を分析することで、従来は予測困難であった地表断層の位置や性状の特定が可能となり、危険地帯における構造物の破壊や人的被害を軽減することが期待される。

**Key Words:** *Applied Element Method, AEM, active fault, dip-slip fault, surface rupture, Ji-Ji earthquake, Kocaeli earthquake*

## 1. INTRODUCTION

Two enormously disastrous earthquakes hit the globe in 1999. The first one was an earthquake of magnitude 7.4 (Mw) occurred in Turkey on 17<sup>th</sup> August 1999<sup>1)</sup>, and immediately following that, another event of magnitude 7.3 (Mw, Central Weather Bureau, Taiwan) occurred in Taiwan on 21<sup>st</sup> September 1999<sup>2)</sup>. Both events caused immense loss to property and lives. The earthquake fault (North Anatolian Fault) in Turkey was traced over 100 km. The magnitude of right lateral movement of the fault on the ground surface was measured to be 2 to 4 m. Normal faults, which were caused secondarily, sunk huge area by a depth of 2-3 m. And in Taiwan, severer effects were observed. The earthquake fault (Cher-Lung-Pu Fault) was traced for about 80 km, here the fault movement directly caused severe damage. The magnitude of maximum vertical differential movement was measured to be nearly 10.0 m as shown in Fig.1. Though these earthquakes were tragic, also provided us the momentum to the process of improvement in understanding the behaviour of nature. From the above two events, it is clear that the severe damage can be caused not

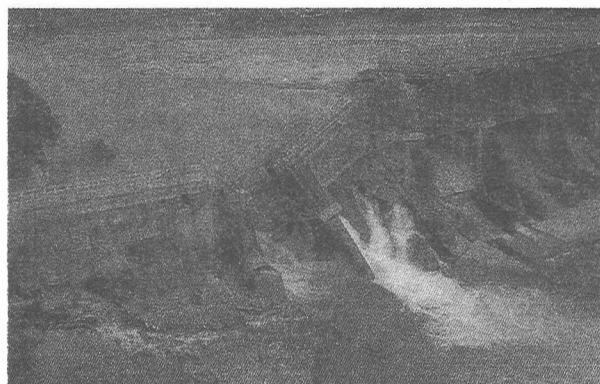
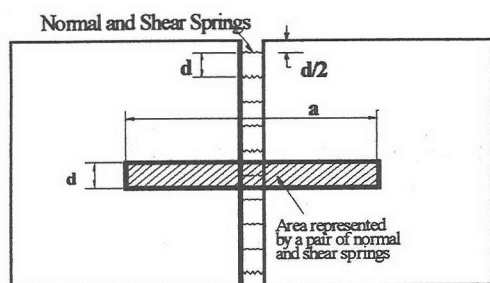
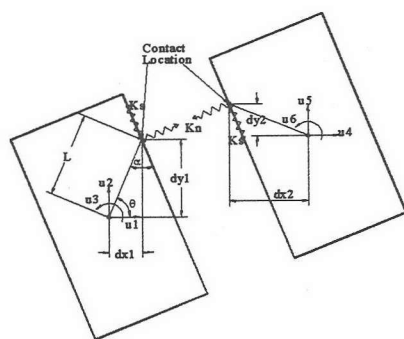


Fig. 1. About 10 m vertical displacement is seen at the Shih-Kang dam site, Taiwan

only by the strong ground motion but also due to large surface deformations lying directly over the seismic faults. Hence, it is necessary to direct our efforts to study the relation between seismic fault characteristics, thickness of soil deposit and surface deformation. Many researchers conducted



(a) Element formulation in AEM



(b) Spring connectivity

Fig. 2. Element modelling in AEM

experiments to understand the phenomena of surface failure, Cole and Lade<sup>3)</sup> have tried to determine the location of surface fault rupture and width of the affected zone in alluvium over dip-slip fault using fault test box. Lade et al.<sup>4)</sup> studied to determine the multiple failure surfaces by conducting the experiments on sand using fault test box. Onizuka et al.<sup>5)</sup> have modelled the deformation of ground using aluminium rods. Through experiments, they investigated bedrock stresses induced by reverse dip-slip faults. Using the above experimental methods, we can find the influence length. However, replicating the actual field conditions using experiments is very difficult, especially, controlling the material properties and modelling the boundary conditions. Moreover, large amount of data is necessary to establish a relationship between seismic fault parameters and resulting surface deformation. On the other hand, studying this phenomenon using numerical model has the advantage of controlling the parameters like material properties, size of the model, boundary condition, dip angle, etc.

## 2. ELEMENT FORMULATION

Applied Element Method (AEM)<sup>6-8)</sup>, which was developed recently as a general method

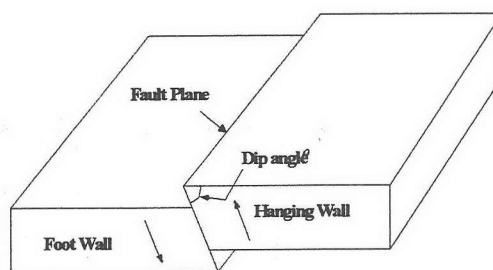


Fig. 3. Fault terminology

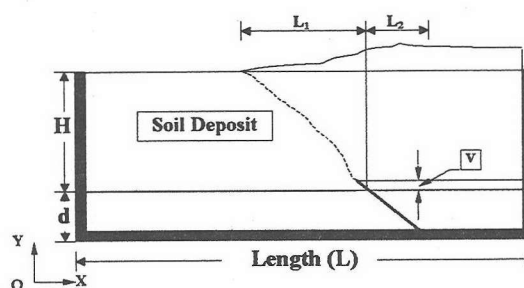


Fig. 4. Fault model

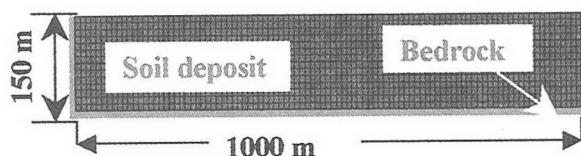


Fig. 5. Numerical model

for structural analysis in both small and large deformation ranges has shown good accuracy in predicting the structural behaviour from no loading till the complete collapse. In AEM, the media is modelled as an assembly of small elements which are made by dividing the structure virtually. Two elements shown in Fig. 2 (a) are assumed to be connected by pairs of normal and shear springs set at contact locations which are distributed around element edges. Stresses and strains are defined based on the displacements of the spring end points. Three degrees of freedom are assumed for each element in 2 dimensional model as shown in Fig. 2 (b). By using the advantage of AEM's simplicity in formulation and accuracy in non-linear range, fault rupture zone shown in Fig. 3 is modelled.

The mechanism as shown in Fig. 3 is called Reverse Dip-Slip Faulting. This is one of the types of faults where the hanging wall moves

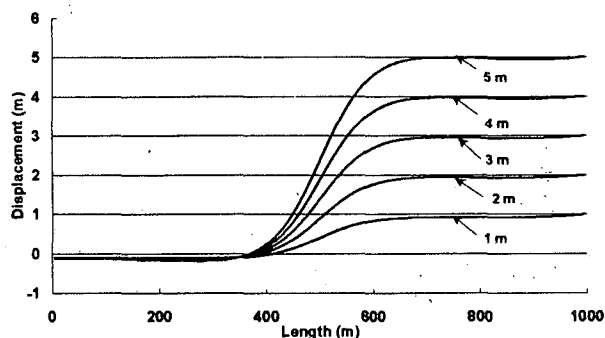


Fig. 6. Surface displacement at each 1-m displacement of hanging wall  
(Case 1: elastic analysis, dip angle =  $90^\circ$ )

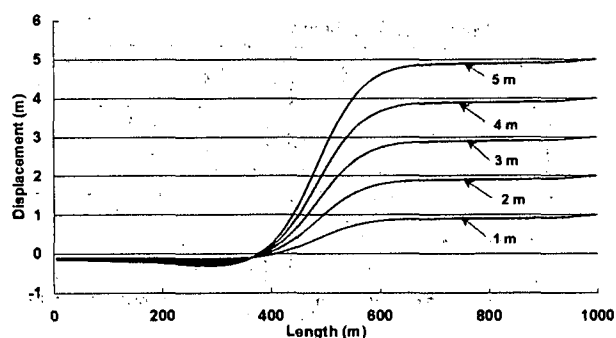


Fig. 8. Surface displacement at each 1-m displacement of hanging wall  
(Case 2: elastic analysis, dip angle =  $45^\circ$ )

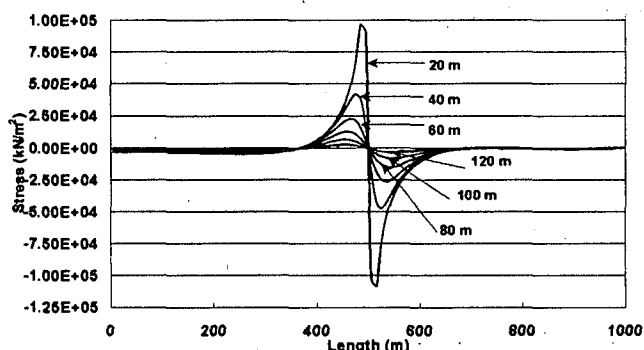


Fig. 7. Stresses in vertical direction in soil deposit at regular intervals (Case 1)

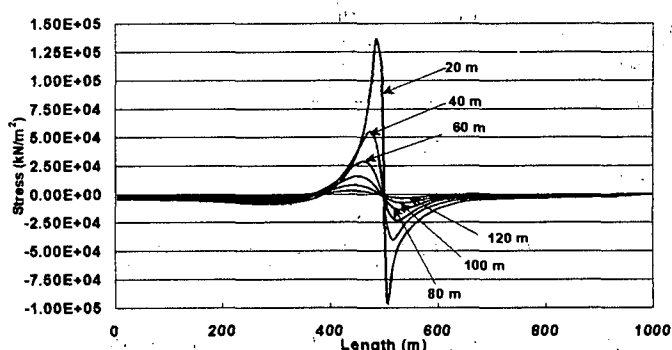


Fig. 9. Stresses in vertical direction in soil deposit at regular intervals (Case 2)

upward relative to the footwall. If the direction of the movement of the hanging wall is downward then it is called normal faulting. In the study discussed in this paper, both normal and reverse dip-slip faults are considered. To analyse the mechanism of fault rupture zone near dip-slip faults, the model shown in Fig. 4 was prepared. In this numerical model, soil deposit of thickness,  $H$  ( $=140$  m), is assumed to be overlay on the bedrock. The length of the model,  $L$ , is assumed as 1,000 m (Fig. 5). Influence lengths,  $L_1$  and  $L_2$ , in Fig. 4, on the surface towards left and right side of the point exactly above the seismic fault, respectively, are calculated by giving the hanging wall a displacement along the direction of dip angle.

### 3. BOUNDARY CONDITION

Generally, soil strata and bedrock extend upto tens of kilometres in horizontal direction. Numerical modelling of such a large media is a difficult task and moreover, for studying the surface behaviour near the

Table 1. Material Properties

	$E$ ( $\text{kN/m}^2$ )	$\gamma$ ( $\text{kN/m}^3$ )
Bedrock	$66 \times 10^6$	26.5
Soil deposit	$20 \times 10^5$	18.0

active fault region, it is necessary to model the small portion of the region which will include all the effects when the bedrock moves. For studying the selected region numerically, we need to assume an appropriate boundary condition such that it will not affect the numerical results greatly. Since the present formulation is done for static case, we assume the boundary on left side to be fixed in horizontal direction, and free to move in vertical direction and can rotate. In order to avoid the interference of boundary condition on numerical results, left side boundary is kept at sufficient distance from the fault zone. The Bottom of the bedrock is assumed as fixed. We think that

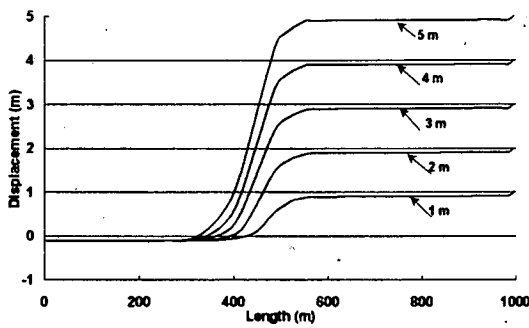


Fig. 10. Surface displacement  
(Case 3a: dip angle =  $90^\circ$  reverse fault)

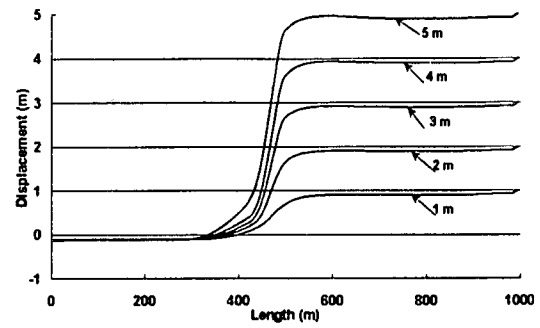


Fig. 12. Surface displacement  
(Case 3b: dip angle =  $45^\circ$  reverse fault)

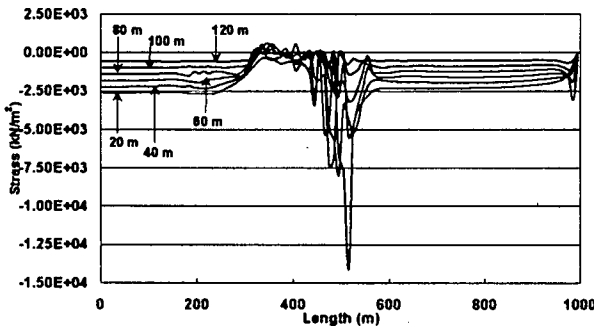


Fig. 11. Stresses in soil deposit (Case 3a)

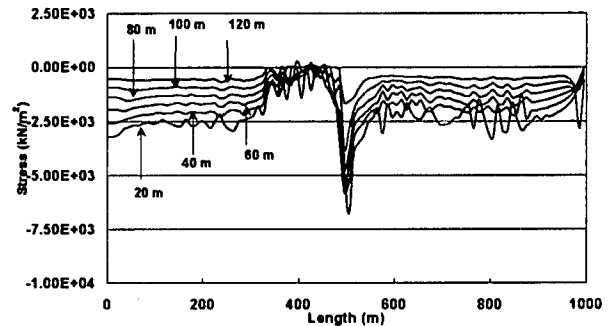


Fig. 13. Stresses in soil deposit (Case 3b)

this kind of boundary condition is appropriate for this problem because more emphasis is given to the near fault behaviour of the formulated model. In case of dynamics, modelling of radiation condition is very important and the boundary condition discussed here can be easily replaced by viscous boundary condition or transmitting boundary<sup>9</sup>.

#### 4. ELASTIC ANALYSIS

To verify the proposed model, analysis is carried out in elastic case by assuming two different dip angles. In Case 1, dip angle is assumed as  $90^\circ$  and in Case 2, it is assumed as  $45^\circ$ . Density and Young's modulus of bedrock and soil deposit are assumed as shown in Table 1. In Case 1, analysis is carried out by giving a displacement of 5 m to hanging wall in vertical direction. Displacement on the surface is plotted in Fig. 6, for every 1-m displacement of the hanging wall. From this figure, it can be understood that the hanging wall portion on the surface is lifted in proportion to the hanging wall displacement. Figure 7 shows stresses in vertical direction taken along the horizontal lines at different depths in soil deposit. Here stresses show high values near the zone of rupture. As we can see

clearly from the figure, the stresses are reducing

Table 2. Material Properties

	$E$ ( $\text{kN/m}^2$ )	$\gamma$ ( $\text{kN/m}^3$ )	$f_c$ ( $\text{kN/m}^2$ )	$f_t$ ( $\text{kN/m}^2$ )
Bedrock	$66 \times 10^6$	26.5	$2.5 \times 10^4$	$2.5 \times 10^3$
Soil deposit	$20 \times 10^5$	18.0	$1.5 \times 10^4$	$1.5 \times 10^3$

when we move near to the surface.

In Case 2, since the dip angle is  $45^\circ$ , analysis is carried out by giving a displacement of 5 m to hanging wall both in vertical and horizontal directions. This means that the hanging wall is moving along the direction on dip angle. Displacement on the surface is plotted Fig. 8, for every 1-m displacement of the hanging wall in horizontal and vertical direction. From Fig. 8 also, it can be understood that the hanging wall portion on the surface is lifted in proportion to the hanging wall displacement. In this figure, we can observe the effect of horizontal movement of hanging wall between 500 m to 600 m. In Fig. 9, stresses in vertical direction taken along the horizontal lines at different heights in soil deposit are plotted. Here also stresses show high values near the zone of rupture. As we can see clearly from the figure, that the stresses are reducing when we move near to the surface.

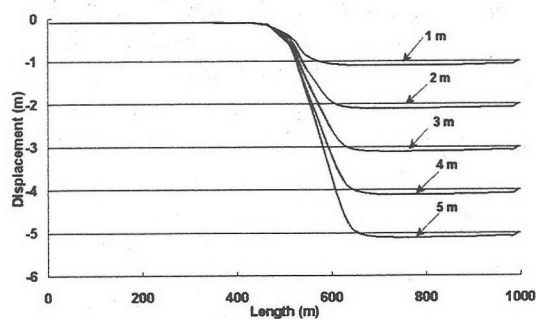


Fig. 14. Surface displacement  
(Case 4a: dip angle =  $90^\circ$  normal fault)

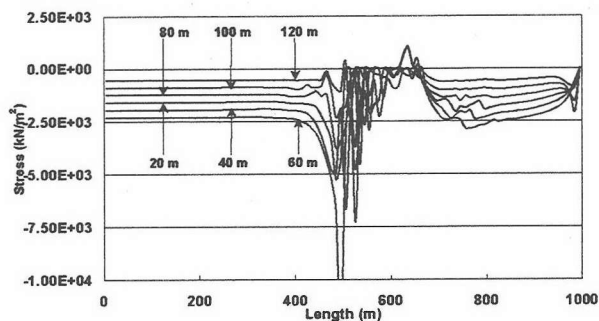


Fig. 15. Stresses in soil deposit (Case 4a)

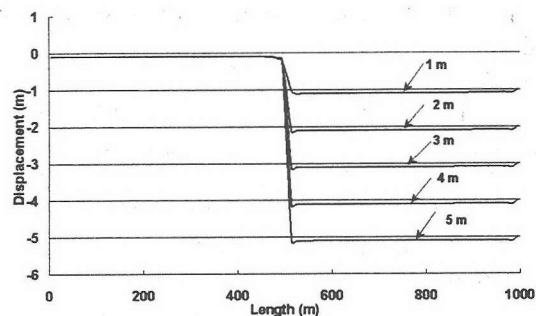


Fig. 16. Surface displacement  
(Case 4b: dip angle =  $45^\circ$  normal fault)

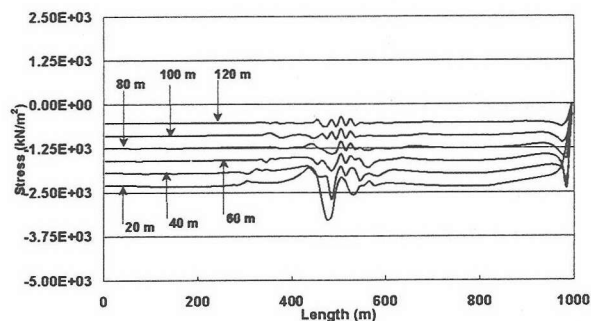


Fig. 17. Stresses in soil deposit (Case 4b)

## 5. NON-LINEAR ANALYSIS

Analysis is carried out for two cases. The first case (Case 3) shown in Figs. 10, 11, 12 and 13 is reverse faulting where hanging wall is moving in upward direction and the stresses in the soil deposit are compressive and the second case (Case 4) shown in Figs. 14, 15, 16 and 17 is normal faulting where the hanging wall is moving in down ward direction and the stresses in the soil deposit are tensile. The displacement on the surface is plotted

for every 1-m displacement of the hanging wall along the direction of dip angle. Material properties for bedrock and soil deposit in case of non-linear analysis are shown in Table 2. Figures 10 and 11 show the displacement and internal stresses for dip angle  $90^\circ$  reverse faulting respectively. From the figures, it can be observed that the displacement on the hanging wall side is in proportion to the movement of the hanging wall movement and the affected zone is concentrated near the fault region only. From Fig. 11, it can be seen that the stress near the zone of rupture are high and these stresses are reducing when we move

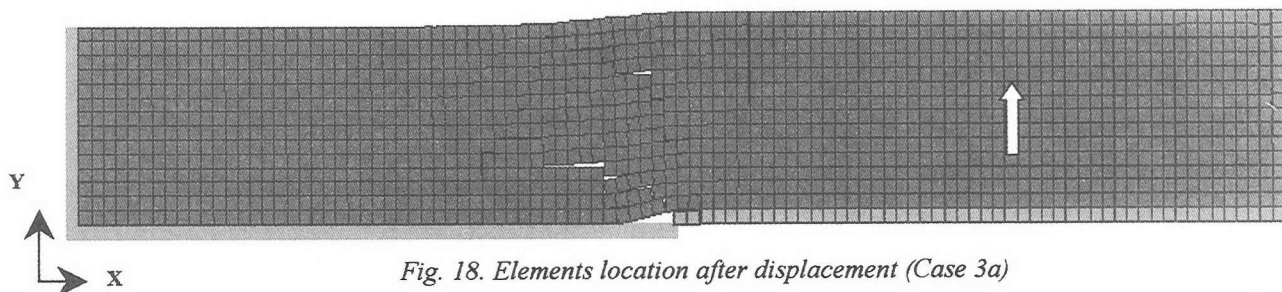


Fig. 18. Elements location after displacement (Case 3a)

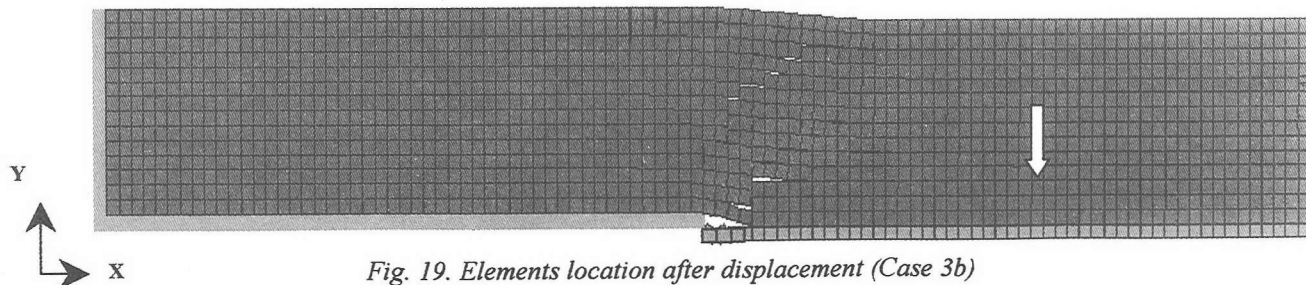


Fig. 19. Elements location after displacement (Case 3b)

towards the surface. Figures 12 and 13 show surface displacement and internal stresses for dip angle  $45^{\circ}$  reverse faulting, respectively. From the surface displacement in Fig.12 the effect of dip angle can be seen. Due to the change in dip angle the influence length has increased. Figures 14 and 15 shows the surface displacement and internal stresses for dip angle  $90^{\circ}$  normal faulting. In this case, hanging wall is moving in downward direction creating the tensile stresses in the bedrock. From Fig. 14, we can easily observe that the influence length is shorter than that in the case of reverse faulting. Figure 15 shows the stress distribution at regular intervals in soil deposit. From this figure, it is clear that the stresses are concentrated near the zone of faulting. Figures 16 and 17 are similar to Figs. 14 and 15 respectively, except for the case of dip angle. Figures 18 and 19 show the elements location after the final displacement for  $90^{\circ}$  normal and reverse faulting respectively. From these figures, we can observe the propagation of cracks from the bedrock to the surface.

This kind of study is necessary to establish the possible locations of the faults appearing on the surface due to future earthquakes because engineers are more concerned about the damage that might be caused when the structures are located on the vulnerable area. According to seismological point of view, some difference between the real fault and the expected fault line is acceptable but for the engineers, this difference might be sometimes of a major concern. Moreover, from the recent earthquakes, it was observed that the structures which are located very near to the zone of faulting have survived and the structures which are far have experienced major damage (JSCE (1999, a) and b)). This shows that there is a strong relation between site conditions and the dynamic characteristics of wave motion. Hence it is important to study the surface behaviour based on the local soil conditions and fault characteristics. This kind of study is difficult to perform experimentally because it is difficult to prepare a model similar to actual case. On the other hand, numerical models which can predict the behaviour of the media accurately in small and large deformation range and in non-linear range have the advantage of modelling any kind of soil and flexibility to change the parameters such as strength of soil, thickness of the deposit and dip angle.

## 6. CONCLUSIONS

A new application of Applied Element Method is proposed in this paper. A dip-slip fault zone is modelled numerically to study the influence of dip angle, bedrock displacement and the thickness of the soil deposit on the length of affected zone. Since this is preliminary model, dynamic aspects such as ground motion, slip rate of fault movement, etc, are not taken into consideration. The boundary condition discussed here can be improved for qualitative discussion since there will be some movement in the horizontal direction along the boundary. Although the discussion done here is for the static case, the method can be extended to dynamic case such as modelling of the unbounded media for studying more realistic phenomenon like wave propagation and dependence on soil parameters.

## REFERENCES

- 1) Japan Society of Civil Engineers, *The 1999 Kocaeli earthquake, Turkey, Investigation into damage to civil engineering structures*, Earthquake Engineering Committee, Japan Society of Civil Engineers, 1999 (a).
- 2) Japan Society of Civil Engineers, *The 1999 Ji-Ji earthquake, Taiwan, Investigation into damage to civil engineering structures*, Earthquake Engineering Committee, Japan Society of Civil Engineers, 1999 (b).
- 3) Cole, D. A., Jr., and Lade, P. V., Influence zones in alluvium over dip-slip faults, *Journal of Geotechnical Engineering*, ASCE, Proc. Paper 18788, Vol. 110, No. GT5, pp. 599-615, 1984.
- 4) Lade, P. V., Cole, D. A., Jr., and Cummings David., Multiple failure surfaces over dip-slip faults, *Journal of Geotechnical Engineering*, ASCE, Proc. Paper 18789, Vol. 110, No. GT5, pp. 616-627, 1984.
- 5) Onizuka, N., Hakuno, M., Iwashita, K. and Suzuki, T., Deformation in grounds and bedrock stress induced by reverse dip-slip faults, *Journal of Applied Mechanics*, JSCE, Vol. 2, pp. 533-542, 1999.
- 6) Meguro, K. and Tagel-Din, H., Applied element method for structural analysis: Theory and application for linear materials, *Structural Eng./Earthquake Eng.*, JSCE, Vol. 17, No. 1, 21s-35s, 2000.
- 7) Tagel-Din, H., A new efficient method for nonlinear, large deformation and collapse analysis of structures, Ph.D. thesis, Civil Eng. Dept., The University of Tokyo, 1998.
- 8) Meguro, K. and Tagel-Din H., A new efficient technique for fracture analysis of structures, *Bulletin of Earthquake Resistant Structure Research Center*, Institute of Industrial Science, The University of Tokyo, No. 30, 1997.
- 9) Wolf, J. P. and Song, Ch., *Finite element modeling of unbounded media*, John Wiley & Sons Ltd., Baffins Lane, Chichester, England, 1996.